Growth of carbon octopus-like structures from carbon black in a fluidized bed

Kinshuk Dasgupta[1,2,*], Jyeshtharaj B. Joshi[2,3,*], Bhaskar Paul[1], Debasis Sen[4], and Srikumar Banerjee[3]

[1]Materials Group, Bhabha Atomic Research Centre, Mumbai 400085, India
[2]Department of Chemical Engineering, Institute of Chemical Technology, Matunga, Mumbai 400019, India
[3]Homi Bhabha National Institute, Anushaktinagar, Mumbai 400094, India
[4]Solid State Physics Division, Bhabha Atomic Research Centre, Mumbai 400085, India

ABSTRACT

Carbon octopi like structures have been grown by catalytic conversion of carbon black in a fluidized bed with the help of ferrocene and acetylene. A growth mechanism has been proposed based on small-angle neutron scattering, scanning electron microscope and transmission electron microscope observations. Addition of carbon black primary particles into multiple nuclei of carbon cap on iron particles led the growth of these structures. It was concluded that the pentagon and heptagon defects in the carbon black have important roles in converting the spherical structure into a cylindrical structure.

Keywords: Carbon Octopus, Electron Microscopy, Small Angle Neutron Scattering, Chemical Vapor Deposition, Catalysis.

Article

1. INTRODUCTION

Carbon nano-material, more precisely carbon nanotube (CNT), is one of the most investigated materials in recent years due to its unique properties and potential applications in the electronic industries, in power generation and storage, in biomedical application, in structural and functional composites, etc.[1–9] The bulk production of CNTs in an economic way is the route for feasibility of these applications. Out of different techniques, catalytic chemical vapour deposition (CCVD) in a fluidized bed is the most promising technique for bulk production of this exotic material.[10–13] In this method one needs to fluidize nano-agglomerate particles[13] containing catalysts (generally transition metals or their compounds), using a carrier gas like nitrogen or argon along with a hydro-carbon gas like methane or acetylene. The CNTs grow

on the catalyst containing nano-agglomerate particles by the decomposition of the hydrocarbon. The use of cheap precursors and the reduction in processing steps are the key factors in producing CNTs economically. In order to meet these requirements, we have chosen carbon black (N 330 grade, furnace black) as the nano-agglomerate particle, ferrocene as the catalyst and acetylene as the precursor hydrocarbon. The beauty of carbon black is that it has primary particles of size 30 nm which form agglomerate in the size range of 80 to 120 μm and can be easily fluidized. It does not require any processing prior to fluidization. On the contrary, mesoporous alumina, magnesia and silica that have been reported in the published literature[11–13] as catalyst-support materials for CNT growth, require several steps of processing prior to fluidization. We have produced significant amount of CNTs over carbon black by fluidized bed synthesis. The results have recently been published.[14] Along with bulk production of CNTs we observed that the carbon black itself got converted into carbon-octopus like structures. Octopus type of growth was observed by Huu et al.[15] on graphite

---

*Authors to whom correspondence should be addressed.
Emails: jb.joshi@ictmumbai.edu.in, jbjoshi@gmail.com,
dasguptakinshuk@yahoo.com, kdg@barc.gov.in

Article

supported nickel catalyst by decomposition of ethane and by Pradhan et al.[16] on copper-nickel catalyst by decomposition of camphor. Saavedra et al.[17] have recently reported octopus-like carbon nanofibers using cupronickel catalyst on silicon, which they claim to be useful for applications such as supercapacitor contacts. There are several other significances of this type of conversion from carbon black. Firstly, the substrate material, which otherwise is leached out, is now usable, either separately or along with nanotubes grown from acetylene. Secondly, starting from a low cost carbon black, more valuable fibre-like structures have been obtained, which gives value addition that needs to be quantified. There is a report by Buchholz et al.[18] on the conversion of carbon black into CNT under the influence of an electric field in an arc discharge furnace at a very high temperature (around 3000 °C). They have proposed a two-stage mechanism of the conversion. In the first stage, the growth of short nanotubes is driven by multiaxial tensile stresses that arise from thermal shrinkage. In the second stage, electrostatic forces present in the plasma of the high-temperature arc-furnace, drive the subsequent extension of the short nanotubes to multiple-micron. However, this mechanism is not applicable in a fluidized bed

which operates in the temperature range of 700–1000 °C. In another report Donnet et al.[19] discuss the growth mechanism of CNTs on carbon black in an oxy-acetylene flame. However, their proposed mechanism does not take into account any role of catalyst in the conversion. In this paper we report the synthesis of carbon octopus-like structures in a fluidized bed and also propose a mechanism for conversion of carbon black into these novel carbon structures.

2. EXPERIMENTAL DETAILS

The schematic of the fluidized bed set up used for the present studies is shown in Figure 1. The diameter and the height of the working zone were 65 and 700 mm respectively. A perforated plate of recrystallized alumina was used as the gas distributor. Carbon black was charged inside the furnace at room temperature and was initially fluidized by nitrogen till the temperature of synthesis was reached. At the temperature of synthesis acetylene flow was added to the nitrogen (1:1). The ferrocene was charged inside the pre-heater, which was heated up to 250 °C. At this temperature ferrocene was vapourized and was carried into the furnace by the gas mixture (nitrogen and
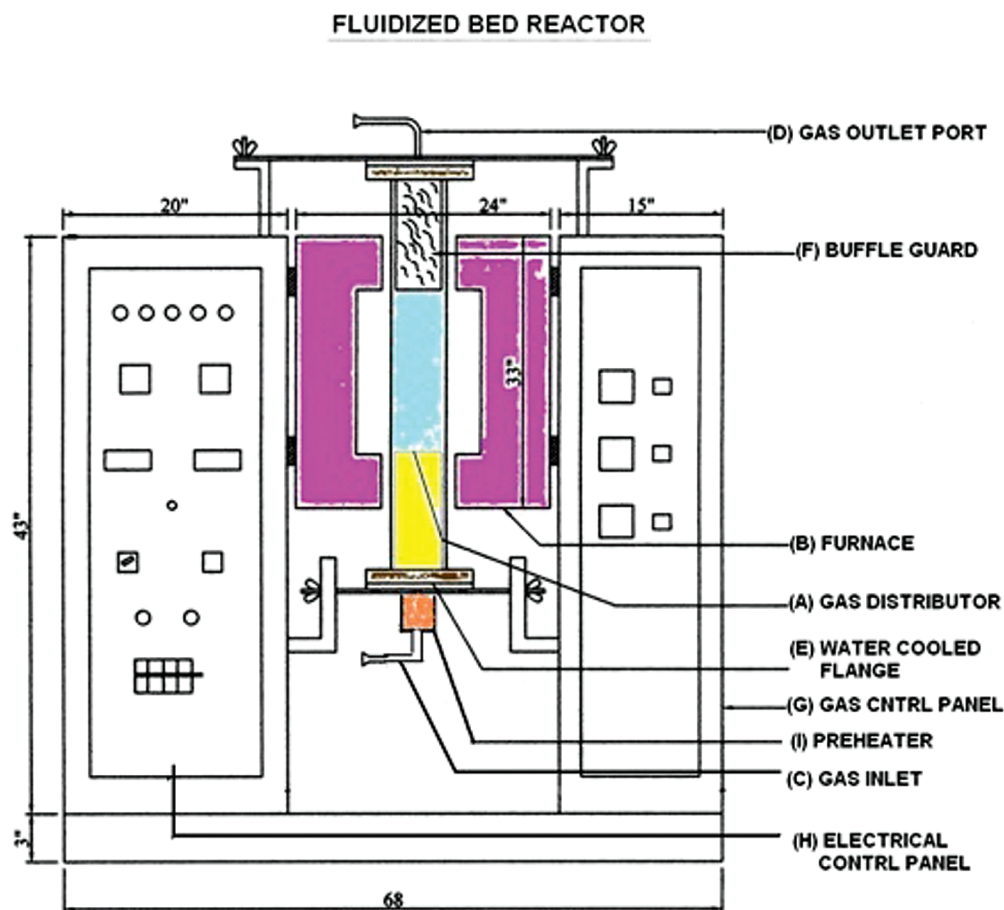

Fig. 1. Schematic of the fluidized bed set up for production of carbon nanotubes.

Growth of carbon octopus-like structures from carbon black in a fluidized bed
Dasgupta et al.

Materials Express

acetylene). Inside the furnace ferrocene gets cracked into Fe nanoparticles and acetylene gets cracked into C and H_2. The pressure drop was measured by a digital manometer. The tapping was done from the inlet and the outlet of the fluidized bed. The minimum fluidization velocity of the carbon black was estimated by measuring the pressure drop across the bed with respect to superficial gas velocity. Three K-type thermocouples for measuring temperature were placed near the distributer, middle and top of the bed, respectively. The experiments were carried out at four different temperatures (700, 800, 900, 1000 °C), three different charges (50, 75, 100 g-corresponding to different bed heights of 60, 90 and 120 mm) and four different time durations (30, 45, 60, 75 minutes). The conversion of acetylene was measured by gas chromatography. The kinetics of carbon naotubes formation has been communicated separately. In this paper we are interested in formation of octopus-like structures.

The products were characterized by scanning electron microscope (SEM-model TESCAN VEGA MV23DDT/40), transmission electron microscope (TEM-model JEOL 2000FX, 200 kV), thermogravimetry (TG-Mettler make), Raman spectroscopy (ISI make) and small angle neutron scattering (SANS).

The carbon deposits obtained after each experiment were subjected to thermogravimetry (TG) analysis. Simultaneous differential scanning calorimetry (DSC) was also performed on the same samples. The deposits were heated in a thermo-balance up to 1000 °C in air at a rate of 5 °C min^{-1}. The weight loss due to oxidation of carbon and the energy released was recorded and analyzed.

SANS experiments have been performed using a double crystal based medium resolution small-angle neutron scattering instrument.[20] The instrument consists of a non-dispersive $(1,-1)$ setting of 111 reflections from silicon single crystals with specimen in-between the two crystals. The scattered intensities have been recorded as a function of wave vector transfer $q[= 4\pi \sin(\theta)/\lambda$, where 2θ is the scattering angle and $\lambda(= 0.312$ nm.) is the incident neutron wavelength for the present experiment]. The specimens under SANS investigations were placed on a sample holder with a circular slit of 1.5 cm. diameter. The measured SANS profiles have been corrected for background and resolution effects.[21]

3. RESULTS AND DISCUSSION

3.1. Fluidization Behaviour

Carbon black has a primary particle size of 30 nm (Fig. 2(a)). However, it forms soft agglomerate of 80–120 μm size (Fig. 2(b)), which helps in fluidization. The carbon black agglomerate shows the fluidization behavior that of Geldart's 'A' group particles. Upon fluidization, initially the bed expands homogeneously and then at a critical gas velocity (U_c) bubbling starts. The minimum fluidization velocity (U_{mf}) and the minimum bubbling velocity (U_c) at room temperature were found to be 2.95 and 5.9 mm/s, respectively. Figure 3 shows the fluidization behaviour of carbon black at room temperature for 50 g sample with increasing gas velocity. The pressure drop at the plateau corresponds to the weight the bed. The synthesis was carried out at $3U_{mf}$.

3.2. Overall Morphology and Characterization of the Products

The SEM images reveal some interesting features of the products. A typical SEM image of the bulk sample, synthesized at 800 °C, is shown in Figure 4(a). If we look at the agglomerates, the structures look like octopi, where from a central point, several number of short carbon nanofibers (octopus legs) of diameter approximately 500–900 nm emerge out like petals of a flower. Around the octopus structure, significant amount of multiwalled carbon nanotubes (MWCNTs) (in the diameter range 40–50 nm) are observed to grow. A close-up SEM image of octopus
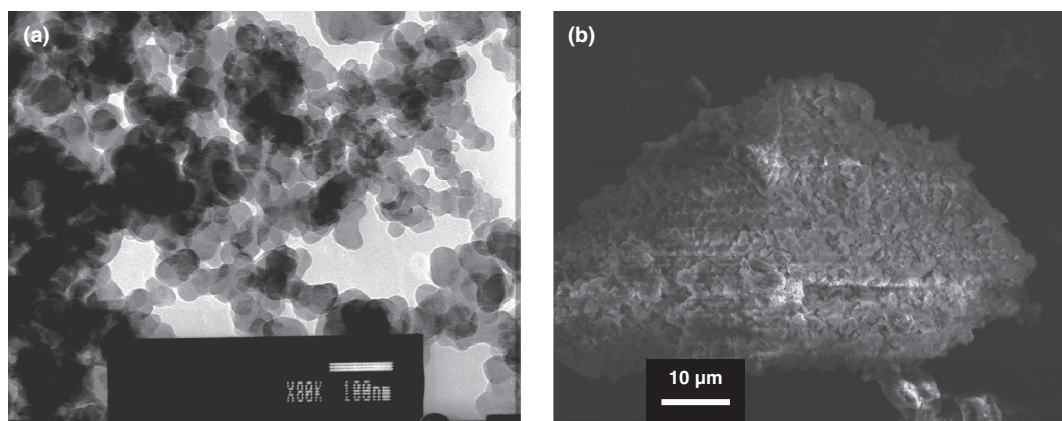
Article

Fig. 2. (a) TEM image of carbon black primary particles. (b) SEM image of carbon black agglomerate.

Materials Express

Growth of carbon octopus-like structures from carbon black in a fluidized bed
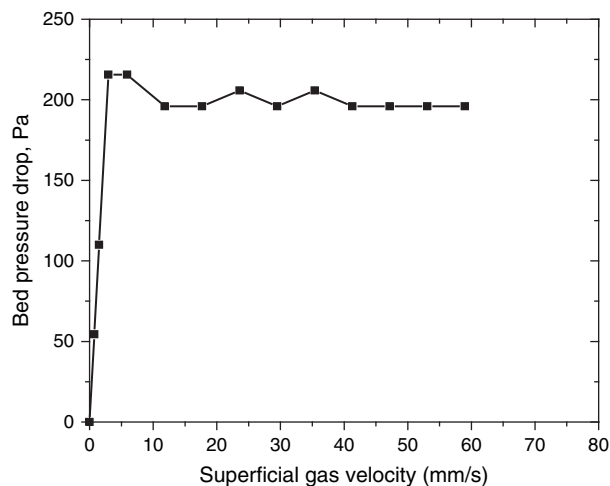Dasgupta et al.

Article

Fig. 3. Variation of bed pressure drop with superficial gas velocity.

structure is shown in Figure 4(b) and that of the MWCNT is shown in Figure 4(c). It has been observed that when the synthesis temperature increases from 700 to 1000 °C, the diameter of the nanofibers decreases but the length increases (Fig. 4(d)). Interestingly, there has been no signature of original carbon black in the final product. It seems, the carbon black agglomerates have converted into octopus-like fibrous structures (500–900 nm) with the help

of the catalyst and acetylene. The MWCNTs (<50 nm) have grown as usual from acetylene over Fe catalyst. The structural details of the MWCNTs can be found in our earlier publication.[14]

The deposit after the synthesis consists of carbon octopi, MWCNTs and catalyst particles. Figure 5(a) shows the TG curve (weight loss with temperature) for deposit at 800 °C (solid line) along with that of original carbon black super-imposed over it (dotted line). For the individual sample, the weight loss starts at a particular temperature (point P and $P^/$ in Fig. 5(a)), which indicates the initiation of oxidation of the carbon deposit. It continues till all the carbon gets burnt (point Q and $Q^/$ in Fig. 5(a)). The residue is the supported catalyst. For the curve PQ, there is no change in slope indicating a single rate of oxidation that of the carbon black. On the other hand there is a change of slope for $P^/Q^/$, indicating two rates of reaction. Figure 5(b) shows the DSC curves of the same samples. DSC curves also show a single peak for carbon black sample and two peaks for the sample synthesized at 800 °C. From Figures 5(a) and (b), it is clear that the oxidation of carbon black starts by 440 °C and gets over by 700 °C. However, there are two oxidation reactions for the carbon deposit synthesized by fluidized bed technique at 800 °C. The first one is for that of the carbon octopi and the second one is for that of the MWCNTs. The oxidation for the CNTs in the deposit starts after 670 °C and continues till 870 °C.
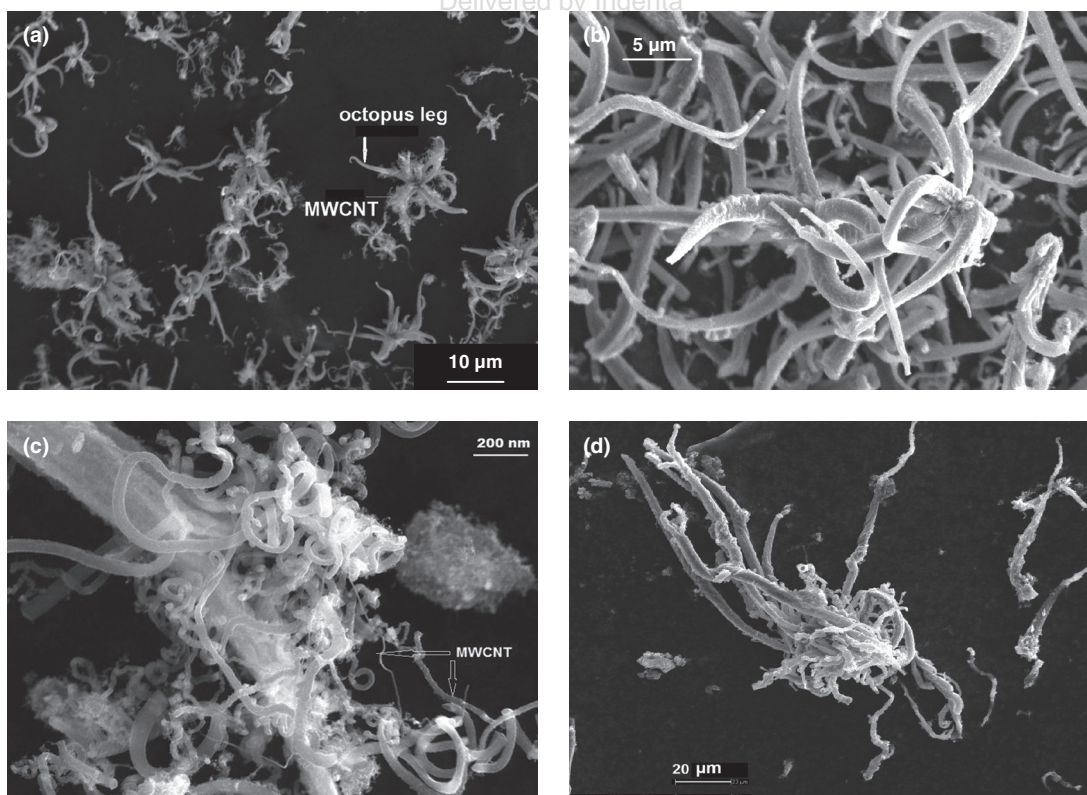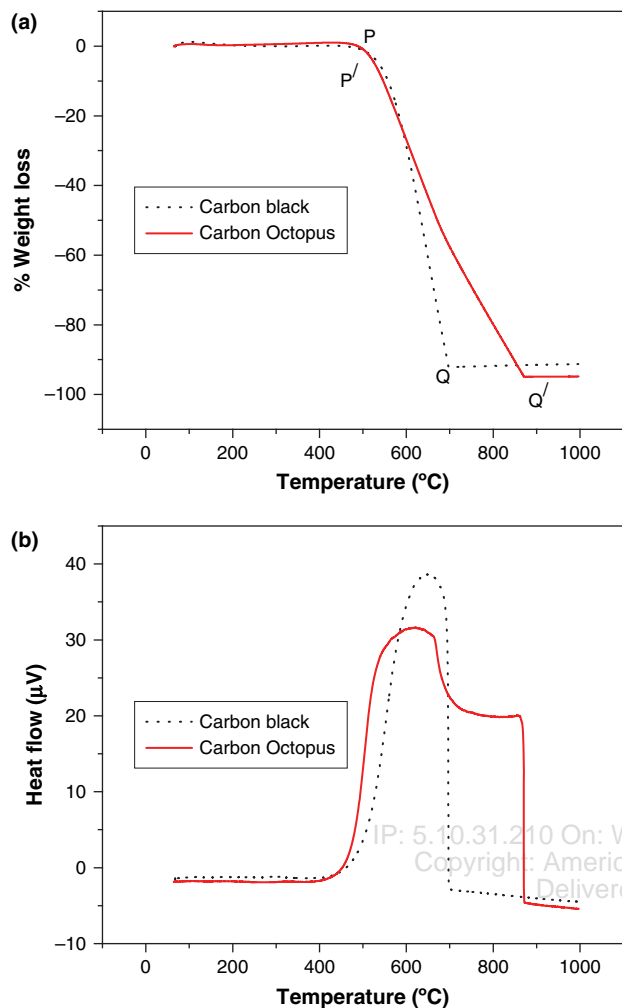
Fig. 4. SEM image of (a) bulk carbon octopus structure produced at 800 °C in the fluidized bed. (b) A single carbon octopus structure showing nanofibers coming out of a point. (c) The MWCNT produced from acetylene over Fe catalyst. (d) Octopus structure produced at 1000 °C

Growth of carbon octopus-like structures from carbon black in a fluidized bed
Dasgupta et al.

Materials Express

(a)

(b)

Fig. 5. (a) TG curves for carbon black and carbon-octopus deposit (synthesized at 800 °C). While the carbon black is showing single rate of oxidation, carbon-octopus deposit is showing two rates of oxidation. (b) DSC curves for carbon black and carbon-octopus deposit (synthesized at 800 °C). The carbon black is showing one exothermic peak but the carbon-octopus deposit is showing two exothermic reactions.

Figure 6 shows the typical Raman spectrum of the sample synthesized at 800 °C. The characteristics 'D' and 'G' peaks are present. 'G' peak corresponds to the zone centre vibration mode of E_{2g} symmetry and 'D' peak originates from the disorder in graphite plane, corresponding to the A_{1g} mode of vibration. Generally in a good quality MWCNT, the intensity of 'D' peak is lesser than that of 'G' peak. Higher intensity of 'D' peak in our sample suggests more disorderedness, which came from octopus-like structure.

3.3. SANS Analysis

The objective of SANS studies was to analyze the average diameter of the carbon fibers (octopus leg) and that of MWCNTs. Electron microscopy can give us result from a
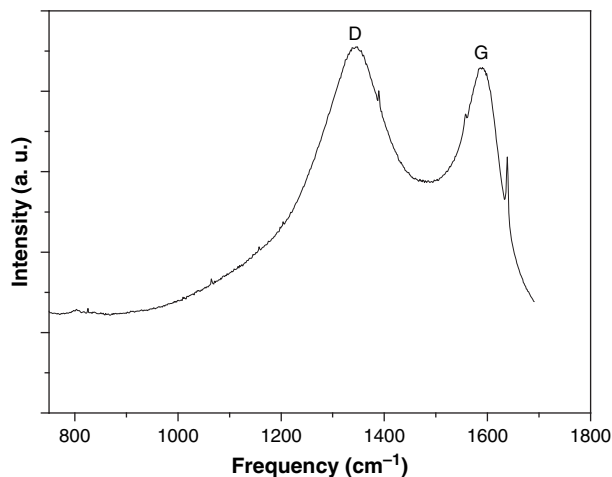
Fig. 6. Raman spectrum for the carbon octopus product synthesized at 800 °C.

small amount of sample. However, SANS data represent the bulk.

As the scattering and real spaces are related by Fourier transform, the scattering signal of neutrons at small angle regime (i.e., at small q regime) contains the information about the mesoscopic density fluctuations (particles). The quantitative information about the morphology of such density fluctuations can be extracted from the analysis of the scattering profile (i.e., from the functional variation of scattering Intensity with q).
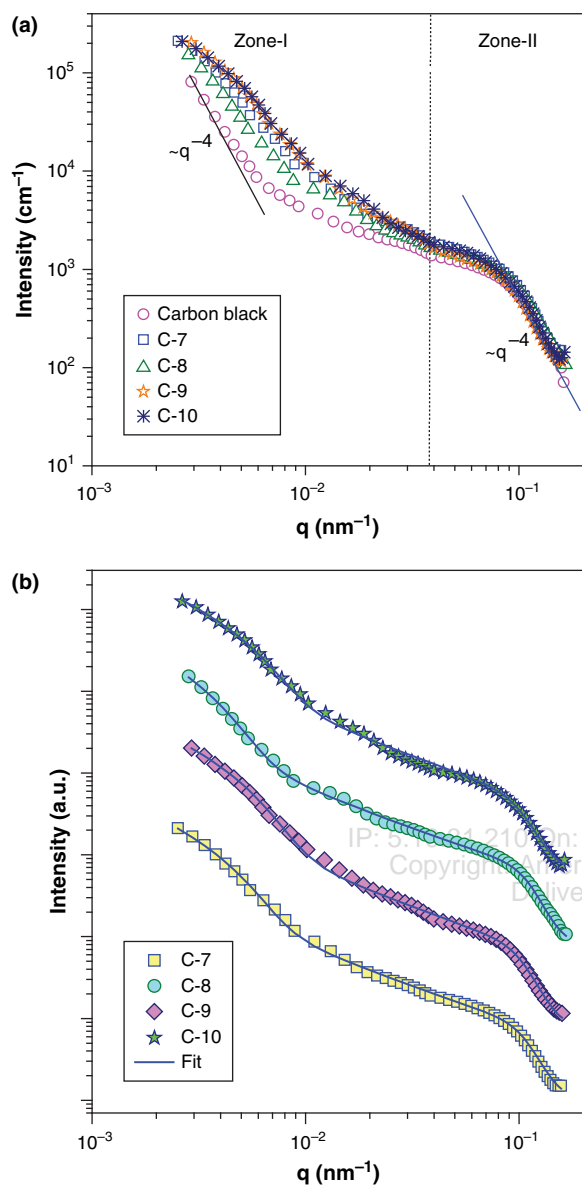
The functionality of the SANS profiles depends on the shape and size of the mesoscopic density fluctuations (particles). From Figure 7(a), it is seen that the SANS profile for each specimen can be broadly categorized in two zones, one below $q < 0.035$ nm^{-1} (Zone-I) and the other above it (Zone-II). It is evident from the figure that for the virgin carbon black sample, the zone-I differs significantly from those after treated at higher temperatures. The functionality of zone-II remains almost unchanged except the functionality of the profiles at the boundary of zones-I and II. The low q part of the zone-I for virgin carbon black sample follows a Porod type (q^{-4}) of behavior.[22] For the treated samples do not follow such behavior. For the Zone-II, there exists a slight shoulder/bending at around q equal to 0.08 nm^{-1} and then a Porod type of behavior is manifested for all the samples. It is worth mentioning that a Porod type of behavior indicates a smooth surface.[22]

As there are mainly two types of cylindrical structures, the SANS intensity for the treated samples has been assumed as the cumulative effect arising from two scattering contributions, i.e.,

$$I_{total}(q) = I_{thick\_cylinder}(q) + I_{thin\_cylinder}(q) \qquad (1)$$

$I_{thick\_cylinder}(q)$ and $I_{thin\_cylinder}(q)$ correspond to scattering contributions from thick nanofibers and thin multiwalled carbon nanotubes, respectively.

$$I_{thick\_cylinder}(q) = \Delta\rho^2 N_{thick\_cylinder} V^2_{thick\_cylinder} P_{cylinder}(q) \quad (2)$$

Article

Materials Express

Growth of carbon octopus-like structures from carbon black in a fluidized bed
Dasgupta et al.

Article

(a)

(b)

Fig. 7. (a) Resolution corrected SANS profile for carbon black and carbon-octopus deposit (C-7 to C-10). (b) SANS data fitted in the appropriate model for the carbon black and carbon-octopus deposit (C-7 to C-10).

$\Delta \rho^2$ is the scattering contrast, $N_{\text{thick\_cylinder}}$ is the number of thick nanofibers, $V_{\text{thick\_cylinder}}$ is the volume of a thick nanofiber and $P_{\text{cylinder}}(q)$ is the form factor of cylinders. For the present case the form factor was expressed according to unified formula.[23]

For the thin nanotubes a similar expression has been adopted. However, an inter-particle correlation term was taken into account in this case as the thin nanotubes are found to very closely spaced and correlated. Therefore,

$$I_{\text{thin\_cylinder}}(q) = \Delta \rho^2 N_{\text{thin\_cylinder}} V^2_{\text{thin\_cylinder}}$$
$$\times P_{\text{cylinder}}(q)S(q) \quad (3)$$

A hard sphere type interaction[24] was assumed for $S(q)$. Radii of the thick and thin cylinders, were estimated from the fitting of the model to the SANS data. Scattering length density was calculated from the scattering length of carbon and nanotube density of 1.3 g/cm³. The fit is depicted in the Figure 7(b).

Table I show that the average diameter of the thick fibers decreases and that of the thin nanotubes increases with increase in synthesis temperature. It also depicts the volumetric ratio of the two types of structures, which randomly varies with temperature. It is to be noted that C-7, C-8, C-9 and C-10 denote the products synthesized at 700, 800, 900 and 1000 °C, respectively.
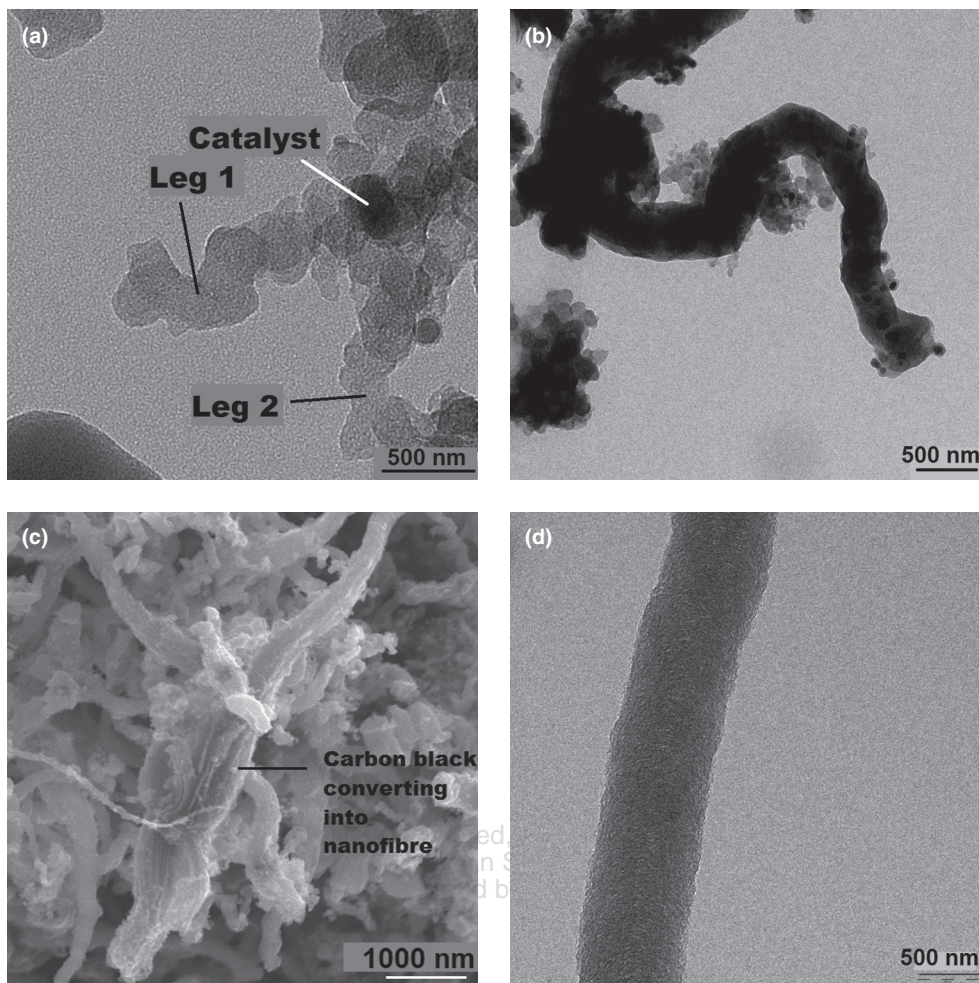
3.4. Evolution of Octopus Structure

In order to find out the evolution of the carbon octopus structure, we collected the samples *in situ* at different intervals of time by inserting Inconel collection pot from the top of the furnace. The samples were analyzed under TEM. Figure 8(a) shows the TEM image after 2 minutes, where the initial growth of octopus legs are depicted. From a central catalyst two legs are coming out. The approximate diameter of the legs ranges between 250–300 nm. Figure 8(b) shows further growth after 8 minutes where the leg has grown further, both in diameter and in length. It has a rough surface with non-uniform diameter. Figure 8(c) is the SEM image of the product after 15 minutes. The arrow in the figure shows the link between carbon black and nanofiber. The detailed structure of the leg is shown in Figure 8(d). There is no hollow core, suggesting it is a fibre with random orientation of graphitic planes. With the help of these figures, we propose the mechanism in the following section.

Conversion of carbon black into carbon octopus-like structure is a significant phenomenon. In the fluidized bed two types of structures have grown. Firstly, CNTs (dia <50 nm) have grown from acetylene over Fe catalyst as happen in a usual fluidized bed process. We have communicated this in our earlier paper[14] and are not discussing here. Secondly, the carbon black has been transformed into octopus-like structure with the help of Fe catalyst and acetylene. The legs of the octopus are carbon nanofibers which are not ordered structures. For transformation of carbon black into octopus-like structure, the presence of acetylene along with ferrocene was necessary. If there

Table I. Average radii of the nanotubes at different temperatures as calculated from SANS data.

Sample	R_{thick} (nm)	R_{thin} (nm)	$(N_{\text{thin\_cylinder}} V^2_{\text{thin\_cylinder}})/(N_{\text{thik\_cylinder}} V^2_{\text{thik\_cylinder}})$
C-7	530	25.5	0.18
C-8	430	26.1	0.23
C-9	362	26.7	0.16
C-10	350	26.9	0.21

Growth of carbon octopus-like structures from carbon black in a fluidized bed
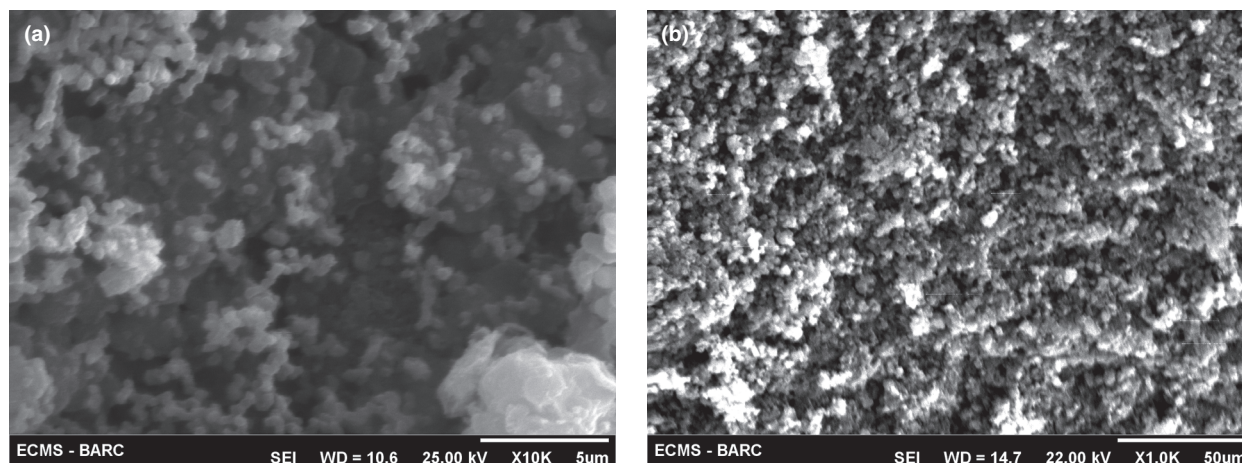Dasgupta et al.

Materials Express

Fig. 8. (a) TEM image of the octopus legs coming out of the Fe catalysts after 2 minutes. The image shows alignment of carbon black primary particles along leg axis. (b) Growth of octopus leg after 8 minutes showing conversion of into carbon nanofiber. (c) SEM image showing an intermediate stage where carbon black is joining the stem of carbon nanofiber. (d) TEM image showing disordered structure of the octopus leg.

was no acetylene supply, there was no transformation. This was verified by conducting an experiment without supplying acetylene where we did not find any transformation (Fig. 9(a)). Similarly, when there was no ferrocene, carbon black did not convert into carbon octopus structure (Fig. 9(b)).

3.5. Growth Mechanism

In order to find out the mechanism of the growth of carbon octopus structures from carbon black, let us first understand the basic structure of carbon black. Carbon black is an aggregate of carbon-onion like structures, built up by concentric carbon-layers around a defect-fullerene nucleus (see Fig. 10).[18, 25] This structure requires a large number of pentagon and heptagon defects to be present in the graphene lattice. The insertion of a pentagon into a hexagonal network introduces positive curvature to the graphene structure[26] and the insertion of a heptagon into a hexagonal network introduces negative curvature to

the graphene structure.[27, 28] Although the insertion of a pentagon–heptagon pair (5–7) into a hexagonal network introduces no net curvature the pair results in many topological features.[29] The double (5–7) defects are in equilibrium with the graphene lattice both in the carbon black and in the nanofibers, by (6–6–6–6) to (5–7–7–5) Stone–Wales transformations (see Fig. 11).[18] The (5–7) defects migrate thermally and at random, both in the carbon black and in the nanofibers, but become concentrated at locations that are energetically favorable. It is known that an energetically-favorable location is the stem of a nanofiber under tensile strain. The activation energy for this transformation is 2.35 eV. The higher concentration of (5–7) defects in the stem increases the probability of interactions between them, that result in the self-annihilation defects by a (5–7–7–5) to (6–6–6–6) reverse Stone–Wales transformation. This causes net migration of (5–7) defects to the stem, and subsequent generation of hexagons in the stem, resulting in the lengthening of the stem.[18]

Materials Express

Growth of carbon octopus-like structures from carbon black in a fluidized bed
Dasgupta et al.

Fig. 9. SEM image of the product synthesized (a) in absence of acetylene (b) in absence of ferrocene showing no existence of octopus-like structures.

In our opinion, in the fluidized bed there is a continuous break and make of carbon black agglomerates into primary nanoparticles. The acetylene after decomposition over Fe nanoparticles forms carbon molecules. These carbon molecules get dissolved into Fe nanoparticles and carbon nanocaps come out of Fe nanoparticles by supersaturation-precipitation process which is already explained in literature.[30–32] These caps are nuclei for further growth. Once the nuclei are formed, primary carbon black particles join the nuclei and grow in length through Stone-Wales transformation mechanism. The formation of either MWCNT or octopus structure depends on the size of the catalyst. When Fe particle size is less than 50 nm it catalyzes MWCNT. When the Fe nanoparticles coalesce into bigger size inside fluidized bed, multiple nucleations from a single catalyst lead to octopus like structure. A schematic of the process is shown in

Figures 12(a–d). The back-scattered electron (BSE) image of the octopus structure is shown in Figure 13, where bigger size Fe catalysts can be seen at the octopus root and smaller Fe catalysts can be seen distributed over CNT products.
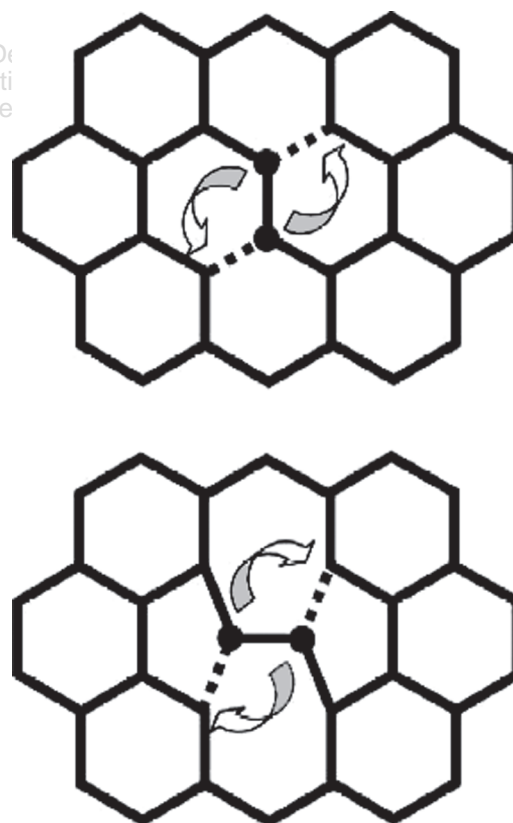
Fig. 11. Formation of a (5–7)-pair defect from four hexagons by a Stone–Wales transformation and the annihilation of a (5–7)-pair defect to form four hexagons by a reverse Stone–Wales transformation (Reproduced with permission from Ref. [18], D. B. Buchholz et al., *Carbon* 41, 1625 (2003). © 2003, Elsevier)
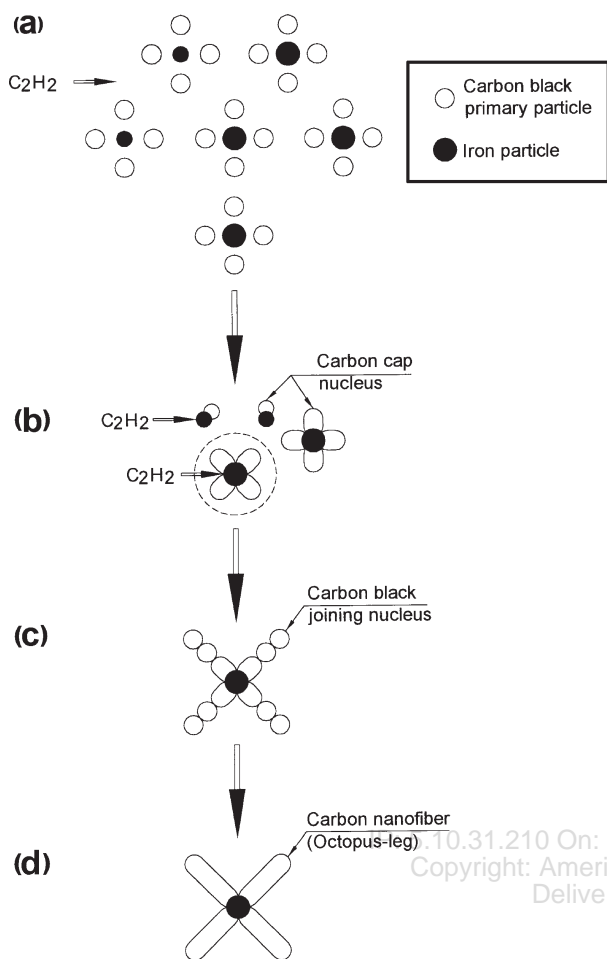

Fig. 10. Schematic of a carbon black structure (Reproduced with permission from Ref. [18], D. B. Buchholz et al., *Carbon* 41, 1625 (2003). © 2003, Elsevier).

Growth of carbon octopus-like structures from carbon black in a fluidized bed
Dasgupta et al.

Materials Express

Fig. 12. Schematic of the growth of carbon octopus structure: (a) Distribution of carbon black primary particles and Fe particles in the fluidized bed. Fe particles have smaller particles and bigger particles. (b) Acetylene is cracking on smaller Fe particle and making single carbon cap nucleus whereas multiple carbon cap nuclei are formed on bigger Fe particles. (c) Primary carbon black particles join the multiple nuclei axis. (d) The carbon nanofibers (octopus legs) are formed by Stone–Wales transformation mechanism.
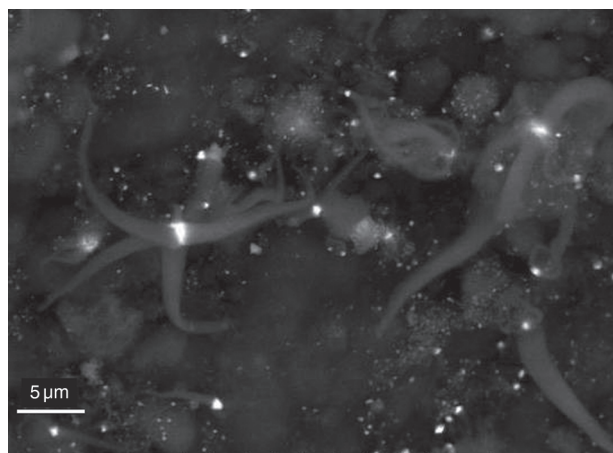
Fig. 13. BSE image showing bigger Fe catalyst sitting at the root of octopus structure and smaller Fe particles are associated with MWCNTs.

From application point of view, carbon octopus-like structure has tremendous potential. If added in a composite it will improve the fracture strength due to its unique structure. It can be used as support material in catalysis due to its high surface area. Its conductivity will be much higher than the original carbon black. Definitely the structure is a value addition to the cheap substrate material, which otherwise is discarded in CNT synthesis.

4. CONCLUSIONS

We have reported here the growth of carbon octopus-like structures from carbon black while producing CNTs in a fluidized bed by CCVD of acetylene over ferrocene. Acetylene has a role of nucleating the seeds of carbon caps on Fe nano-particles, responsible for growth of tubular structures. The possible growth mechanism has been proposed as the transformation of pentagon–heptagon defect pairs of carbon black into hexagon–hexagon pairs added to the available nuclei. The transformation of carbon black into carbon octopus-like structure is significant from commercial and application point of view.

References and Notes

1. R. H. Baughman, A. A. Zakhidov, and W. A. de Heer; Carbon nanotubes—the route toward applications; *Science* 297, 781 (**2002**).
2. J. M. Bonard, H. Kind, T. Stockli, and L. O. Nilsson; Field emission from carbon nanotubes: The first five years; *Solid State Electron.* 45, 893 (**2001**).
3. A. C. Dillon, K. M. Jones, T. A. Bekkedahl, C. H. Kiang, D. S. Bethune, and M. J. Heben; Storage of hydrogen in single-walled carbon nanotubes; *Nature* 386, 377 (**1997**).
4. J. P. Fan, D. M. Zhang, D. Q. Zhao, G. Zhang, M. S. Wu, F. Wei, and Z. J. Fan; Toughening and reinforcing alumina matrix composite with single-wall carbon nanotubes; *Appl. Phys. Lett.* 89, 121910 (**2006**).
5. S. J. Tans, M. H. Devoret, H. J. Dai, A. Thess, R. E. Smalley, L. J. Geerligs, and C. Dekker; Individual single-wall carbon nanotubes as quantum wires; *Nature* 386, 474 (**1997**).
6. K. Tsukagoshi, N. Yoneya, and S. Uryu; Carbon nanotube devices for nanoelectronics; *Physica B* 323, 107 (**2002**).
7. T. Fujimori, S. Tsuruoka, B. Fugetsu, S. Maruyama, A. Tanioka, M. Terrones, M. S. Dresselhaus, M. Endo, and K. Kaneko; Enhanced x-ray shielding effects of carbon nanotubes; *Mater. Express* 1, 273 (**2011**).
8. S. Ishii, S. Kishimoto, Y. Ohno, and T. Mizutani; Air-free fabrication and investigation of effect of air exposure on carbon nanotube field-effect transistors; *Mater. Express* 1, 285 (**2011**).
9. Y. Y. Huang, J. E. Marshall, C. Gonzalez-Lopez, and E. M. Terentjev; Variation in carbon nanotube polymer composite conductivity from the effects of processing, dispersion, aging and sample size; *Mater. Express* 1, 315 (**2011**).
10. K. Dasgupta, J. B. Joshi, and S. Banerjee; Fluidized bed synthesis of carbon nanotubes—a review; *Chem. Eng. J.* 171, 841 (**2011**).

Article

Materials Express

Growth of carbon octopus-like structures from carbon black in a fluidized bed
Dasgupta et al.

Article

11. A. Morancais, B. Caussat, Y. Kihn, P. Kalck, D. Plee, P. Gaillard, D. Bernard, and P. Serp; A parametric study of the large scale production of multi-walled carbon nanotubes by fluidized bed catalytic chemical vapor deposition; *Carbon* 45, 624 (**2007**).

12. R. Philippe, A. Morancais, M. Corrias, B. Caussat, Y. Kihn, P. Kalck, D. Plee, P. Gaillard, D. Bernard, and P. Serp; Catalytic production of carbon nanotubes by fluidized-bed CVD; *Chemical Vapor. Depos.* 13, 447 (**2007**).

13. Y. Wang, F. Wei, G. H. Luo, H. Yu, and G. S. Gu; The large-scale production of carbon nanotubes in a nano-agglomerate fluidized-bed reactor; *Chem. Phys. Lett.* 364, 568 (**2002**).

14. K. Dasgupta, D. Sen, T. Mazumdar, R. K. Lenka, R. Tewari, S. Mazumder, J. B. Joshi, and S. Banerjee; Formation of bamboo-shaped carbon nanotubes on carbon black in a fluidized bed; *J. Nanopart. Res.* 14, 728 (**2012**).

15. C. P. Huu, R. Vieira, B. Louis, A. Carvalho, J. Amadou, T. Dintzer, and M. J. Ledoux; About the octopus-like growth mechanism of carbon nanofibers over graphite supported nickel catalyst; *J. Catal.* 240, 194 (**2006**).

16. D. Pradhan, M. Sharon, M. Kumar, and Y. Ando; Nano-octopus: A new form of branching carbon nanofiber; *J. Nanosci. Nanotech.* 3, 215 (**2003**).

17. M. S. Saavedra, G. D. Sims, L. N. McCartney, V. Stolojan, J. V. Anguita, Y. Y. Tan, S. L. Ogin, P. A. Smith, and S. R. P. Silv; Catalysing the production of multiple arm carbon octopi nanostructures; *Carbon* 50, 2141 (**2012**).

18. D. B. Buchholz, S. P. Doherty, and R. P. H. Chang; Mechanism for the growth of multiwalled carbon nanotubes from carbon black; *Carbon* 41, 1625 (**2003**).

19. J. B. Donnet, H. Oulanti, and T. L. Huu; Mechanism growth of multiwalled carbon nanotubes on carbon black; *Diamond and Relat. Mater.* 17, 1506 (**2008**).

20. S. Mazumder, D. Sen, T. Saravanan, and P. R. Vijayaraghavan; Performance and calibration of the newly installed medium resolution double crystal based small angle neutron scattering instrument at Trombay; *J. Neutron Res.* 9, 39 (**2001**).

21. L. A. Feigin and D. I. Svergun; Structure Analysis by Small-Angle X-ray and Neutron Scattering; Plenum Press, New York (**1987**).

22. S. Ciccariello, J. Goodisman, and H. Brumberger; On the Porod law; *J. Appl. Cryst.* 21, 117 (**1988**).

23. G. Beaucage; Approximations leading to a unified exponential/power-law approach to small-angle scattering; *J. Appl. Cryst.* 28, 717 (**1995**).

24. N. W. Aschroft and J. Lekner; Structure and resistivity of liquid metals. *J. Phys. Rev.* 145, 83 (**1966**).

25. V. I. Berezkin; Fullerenes as nuclei of carbon black particles; *Phys. Solid State* 42, 580 (**2000**).

26. A. Krishnan, E. Dujardin, M. M. J. Treacy, J. Hugdahl, S. Lynum, and T. W. Ebbesen; Graphitic cones and the nucleation of curved carbon surfaces; *Nature* 388, 451 (**1997**).

27. S. Iijima, P. Toshinari, and Y. Ando; Pentagons, heptagons and negative curvature in graphite microtubule growth; *Nature* 356, 776 (**1992**).

28. T. Lenosky, X. Gonze, M. Teter, and V. Elser; Energetics of negatively curved graphitic carbon; *Nature* 355, 333 (**1992**).

29. J. C. Charlier, M. Terrones, F. Banhart, N. Grobert, H. Terrones, and P. M. Ajayan; Experimental observation and quantum modeling of electron irradiation on single-wall carbon nanotubes; *IEEE Trans. Nanotechnol.* 2, 349 (**2003**).

30. R. T. K. Baker; Catalytic growth of carbon filaments; *Carbon* 27, 315 (**1989**).

31. R. T. K. Baker, M. A. Barber, P. S. Harris, F. S. Feates, and R. J. Waite; Nucleation and growth of carbon deposits from the nickel catalyzed decomposition of acetylene; *J. Catal.* 26, 51 (**1972**).

32. S. B. Sinnott, R. Andrews, D. Qian, A. M. Rao, Z. Mao, E. C. Dickey, and F. Derbyshire; Model of carbon nanotube growth through chemical vapor deposition; *Chem. Phys. Lett.* 315, 25 (**1999**).